Acta Crystallographica Section D
Biological Crystallography
ISSN 0907-4449

The apo structure of sucrose hydrolase from *Xanthomonas campestris* pv. *campestris* shows an open active-site groove

Elise Champion,[a] Magali Remaud-Simeon,[a] Lars K. Skov,[b] Jette S. Kastrup,[c] Michael Gajhede[c] and Osman Mirza[c]*

[a]Laboratoire d'Ingénierie des Systèmes Biologiques et des Procédés, Toulouse, France, [b]Novozymes A/S, Krogshøjvej 36, DK-2880 Bagsværd, Denmark, and [c]Biostructural Research, Department of Medicinal Chemistry, Faculty of Pharmaceutical Sciences, University of Copenhagen, Universitetsparken 2, 2100 Copenhagen, Denmark

Correspondence e-mail: om@farma.ku.dk

Received 4 September 2009
Accepted 2 October 2009

PDB Reference: sucrose hydrolase, 2wpg, r2wpgsf.

Glycoside hydrolase family 13 (GH-13) mainly contains starch-degrading or starch-modifying enzymes. Sucrose hydrolases utilize sucrose instead of amylose as the primary glucosyl donor. Here, the catalytic properties and X-ray structure of sucrose hydrolase from *Xanthomonas campestris* pv. *campestris* are reported. Sucrose hydrolysis catalyzed by the enzyme follows Michaelis–Menten kinetics, with a K_m of 60.7 m*M* and a k_{cat} of 21.7 s^{-1}. The structure of the enzyme was solved at a resolution of 1.9 Å in the resting state with an empty active site. This represents the first apo structure from subfamily 4 of GH-13. Comparisons with structures of the highly similar sucrose hydrolase from *X. axonopodis* pv. *glycines* most notably showed that residues Arg516 and Asp138, which form a salt bridge in the *X. axonopodis* sucrose complex and define part of the subsite −1 glucosyl-binding determinants, are not engaged in salt-bridge formation in the resting *X. campestris* enzyme. In the absence of the salt bridge an opening is created which gives access to subsite −1 from the 'nonreducing' end. Binding of the glucosyl moiety in subsite −1 is therefore likely to induce changes in the conformation of the active-site cleft of the *X. campestris* enzyme. These changes lead to salt-bridge formation that shortens the groove. Additionally, this finding has implications for understanding the molecular mechanism of the closely related subfamily 4 glucosyl transferase amylosucrase, as it indicates that sucrose could enter the active site from the 'nonreducing' end during the glucan-elongation cycle.

1. Introduction

Glycoside hydrolase family 13 (GH-13; http://www.cazy.org) mainly contains starch-degrading or starch-modifying enzymes that follow an α-retaining mechanism. The enzymes form a covalently bound glycosyl intermediate, which is transferred onto an acceptor molecule. In this intermediate the glycosyl moiety is bound to a catalytic nucleophile (an Asp residue) and the formation and subsequent transfer onto the acceptor is assisted by a catalytic acid/base (a Glu residue). A subset of enzymes from the GH-13 family utilize sucrose instead of amylose as the primary glucosyl donor: sucrose isomerase, sucrose hydrolase (SH), isomaltulose synthase, sucrose phosphorylase and amylosucrase (AS). Sucrose isomerase, isomaltulose synthase and sucrose phosphorylase show little sequence similarity to other GH-13 enzymes and are therefore not placed into any GH-13 subfamily. SHs and ASs cluster with an identity of about 35% and constitute subfamily 4. AS catalyzes the formation of an insoluble α-glucan, with hydrolysis being a very minor side reaction. Owing to their relatively

high sequence identity, it was believed until recently that the SHs in the family had a transferase activity similar to that of AS. Kim and coworkers reported the characterization and structure determination of SH from *Xanthomonas axonopodis* pv. *glycines* (SX) in complex with sucrose, glucose and Tris and showed that this enzyme has exclusively sucrose hydrolytic activity (Kim *et al.*, 2004, 2008). Several structures of AS in complex with inhibitors and substrates have also been solved (Skov *et al.*, 2001, 2002; Mirza *et al.*, 2001; Jensen *et al.*, 2004). At the structural level the two enzymes are very similar and consist of five domains. However, all domains except for the N-domain are found to have varying sizes in several enzymes from the GH-13 family.

The structure of SX in complex with sucrose unambiguously pinpointed the active site of SH (Kim *et al.*, 2008). The catalytic acid is Asp280 and the catalytic base is Glu322. Subsite −1 binds the glucosyl moiety of sucrose, which is subsequently converted into a covalent glucosyl intermediate. The fructosyl moiety is bound in subsite +1. Structural changes are expected to occur upon substrate binding. However, structures of the native apo enzyme have not been available for any SH or AS enzyme until now. Here, we present the catalytic properties and the structure of SH from *X. campestris* pv. *campestris* (SC) in the resting apo state with an empty active site (apo SC), with apo in this context referring to the native enzyme with no ligand present in the active site. This structure provides insight into the sucrose-induced structural rearrangements that occur just before glucosyl-enzyme formation.

2. Materials and methods

2.1. Expression and protein purification

The SC cloning and expression protocol was performed by Protein'eXpert. The XCC3359 gene was amplified by PCR using *LA Taq* polymerase (Takara) with *X. campestris* pv. *campestris* genomic DNA (ATCC) and oligonucleotides (primers XCC3359_forward, 5′-CATCACCATCAATTGATGATCGCTTCCTCCCCCATCGATGC-3′, and XCC3359_reverse, 5′-TCACCATCCACCAATTGTCAACGACGCTGCAACCAGCGCAC-3′; Proligo France) and ligated into expression vector pLX2 (a vector derived by Protein'eXpert from pQE80; Qiagen) to introduce an N-terminal multi-histidine tag (pLX2-SC). *Escherichia coli* TOP10 expression-strain cells containing pLX2-SC were grown at 288 K in LB medium supplemented with 100 µg ml^{-1} ampicillin. Protein expression was induced by the addition of 1 m*M* IPTG at an optical density (at 600 nm; OD_{600}) of 0.6. The cells were harvested after growth for 15 h at 288 K and the pellet was resuspended to a final OD_{600} of 80 in native wash buffer (50 m*M* Tris–HCl, 300 m*M* NaCl pH 7.5). After sonication, the extract was centrifuged and the supernatant was incubated (slow agitation for 1 h at 277 K) with Ni–NTA resin (Qiagen) equilibrated with 50 m*M* Tris–HCl, 300 m*M* NaCl pH 7.5. Unbound material was removed by washing with 50 m*M* Tris–HCl, 300 m*M* NaCl, 20 m*M* imidazole pH 7.5. The fusion protein was eluted with 50 m*M* Tris–HCl, 300 m*M* NaCl, 200 m*M* imidazole pH 7.5. The buffer was subsequently exchanged to Tris buffer (50 m*M* Tris–HCl, 300 m*M* NaCl, 15% glycerol pH 7.5). Assays were performed using 146 m*M* sucrose. One unit of SC activity was defined as the amount of protein that hydrolyzed 1 µmol of sucrose per minute. The fructose and glucose concentrations were determined by the 3,5-dinitrosalicylic acid (DNS) method (Sumner & Howell, 1935). Fructose was used as a reference, as the same amount of fructose and glucose resulted in an almost identical increase in the 540 nm absorption. SC activity was measured at different temperatures (from 293 to 333 K in 5 K intervals) and at different pH values (from 2.5 to 10.5 in 0.5 pH-unit intervals). The optimum enzymatic activity was found to be at 303–308 K and between pH values of 6.7 and 8.3, with a specific activity of 18 U mg^{-1}. The kinetic parameters were determined in the presence of 58 mg l^{-1} purified SC and 5–900 m*M* sucrose in a 2 ml reaction volume. 200 µl samples were taken at regular time intervals (10–15 min) and SC was immediately inactivated by heating (5 min, 358 K). All samples were analyzed by HPLC. The fructose and glucose concentrations were determined using an Aminex HPX-87H carbohydrate-analysis column (Bio-Rad) at 303 K (elution with a H_2SO_4 concentration of 8.5 m*M* at 0.6 ml min^{-1}). The initial rate of sucrose consumed, corresponding to the initial rate of fructose (or glucose) released, was expressed in micromoles of fructose (or glucose) released per minute and per gram of enzyme.

Table 1
Data-collection and refinement statistics.

Values in parentheses are for the highest resolution shell.

Data collection	
Space group	$P2_1$
Unit-cell parameters (Å, °)	a = 71.6, b = 47.7, c = 87.9, α = 90.00, β = 98.35, γ = 90.00
Wavelength (Å)	1.54179
Resolution (Å)	34.9–1.90 (2.00–1.90)
Total reflections	159390 (21309)
Unique reflections	43650 (6011)
Redundancy	3.5 (3.5)
Completeness (%)	93.9 (88.8)
R_{merge}† (%)	7.8 (34.9)
$I/\sigma(I)$	9.3 (2.2)
Refinement	
Resolution (Å)	24.8–1.90 (1.94–1.90)
R factor‡	0.15 (0.17)
R_{free}§	0.20 (0.24)
R.m.s. deviations	
Bond lengths (Å)	0.006
Bond angles (°)	1.0
Dihedral angles (°)	16.0

† $R_{merge} = \sum_{hkl}\sum_i |I_i(hkl) - \langle I(hkl)\rangle| / \sum_{hkl}\sum_i I_i(hkl)$, where $I_i(hkl)$ is the ith measurement. ‡ R factor $= \sum_{hkl} ||F_{obs}| - |F_{calc}|| / \sum_{hkl} |F_{obs}|$. § R_{free} was calculated using 5% randomly selected reflections that were excluded from refinement.

2.2. Crystal structure determination

Purified apo SC was concentrated to 2 mg ml^{-1}. Crystallization took place using the hanging-drop vapour-diffusion method at 277 K by mixing 2.5 µl protein solution with 2.5 µl reservoir solution [30%(*w*/*v*) PEG 6000, 0.1 *M* MES pH 6.3]. Single crystals were mounted in cryo-loops directly from the mother liquor and were frozen in liquid nitrogen. Data were

collected from a single crystal at 120 K on an in-house R-AXIS rotating-anode generator equipped with a MAR 345 detector. Data processing to 1.9 Å resolution was performed using *MOSFLM* and *SCALA* (Leslie, 1992; Evans, 1993). The crystals belonged to the monoclinic space group $P2_1$, with one enzyme molecule in the asymmetric unit. The structure of SC was solved by molecular replacement using the program *Phaser* (McCoy *et al.*, 2007) with a truncated form of the structure of AS (PDB code 1g5a; Skov *et al.*, 2002) as the search model. At the time of data collection no SH structures had been determined. Model building was performed with *Coot* (Emsley & Cowtan, 2004). Refinement was performed using *CNS* and *PHENIX* (Brunger, 2007; Adams *et al.*, 2002). All residues except regions 225–227 and 438–442 (not included in the model) showed good overall density. 860 water molecules were included in the final model. Thr614 was found in a disallowed region of the Ramachandran plot (ADIT validation server; http://deposit.rcsb.org/validate/); however, this conformation seems to be justified by good electron density and is involved in tight hydrogen-bonding networks. Data-collection and refinement statistics are given in Table 1. The structure has been deposited in the Protein Data Bank with PDB code 2wpg.

3. Results and discussion

3.1. Catalytic properties of SC

The reaction products resulting from the action of SC on sucrose as the sole substrate were shown to be exclusively glucose and fructose in an equal molar ratio. The initial rates of sucrose hydrolysis were determined by measuring the release of fructose (or glucose). A double-reciprocal plot (not shown) showed that sucrose hydrolysis by SC follows Michaelis–Menten kinetics, with a K_m of 60.7 mM and a k_{cat} of 21.7 s^{-1}. As shown in Table 2, the turnovers (k_{cat}) of SC and SX are of the same order of magnitude. On the other hand, SC shows a lower affinity for sucrose than SX. In contrast to sucrose hydrolases, amylosucrases, which are polymerases, do not follow classic Michaelis–Menten behaviour for sucrose consumption and display lower turnover (Potocki de Montalk *et al.*, 2000; Pizzut-Serin *et al.*, 2005).

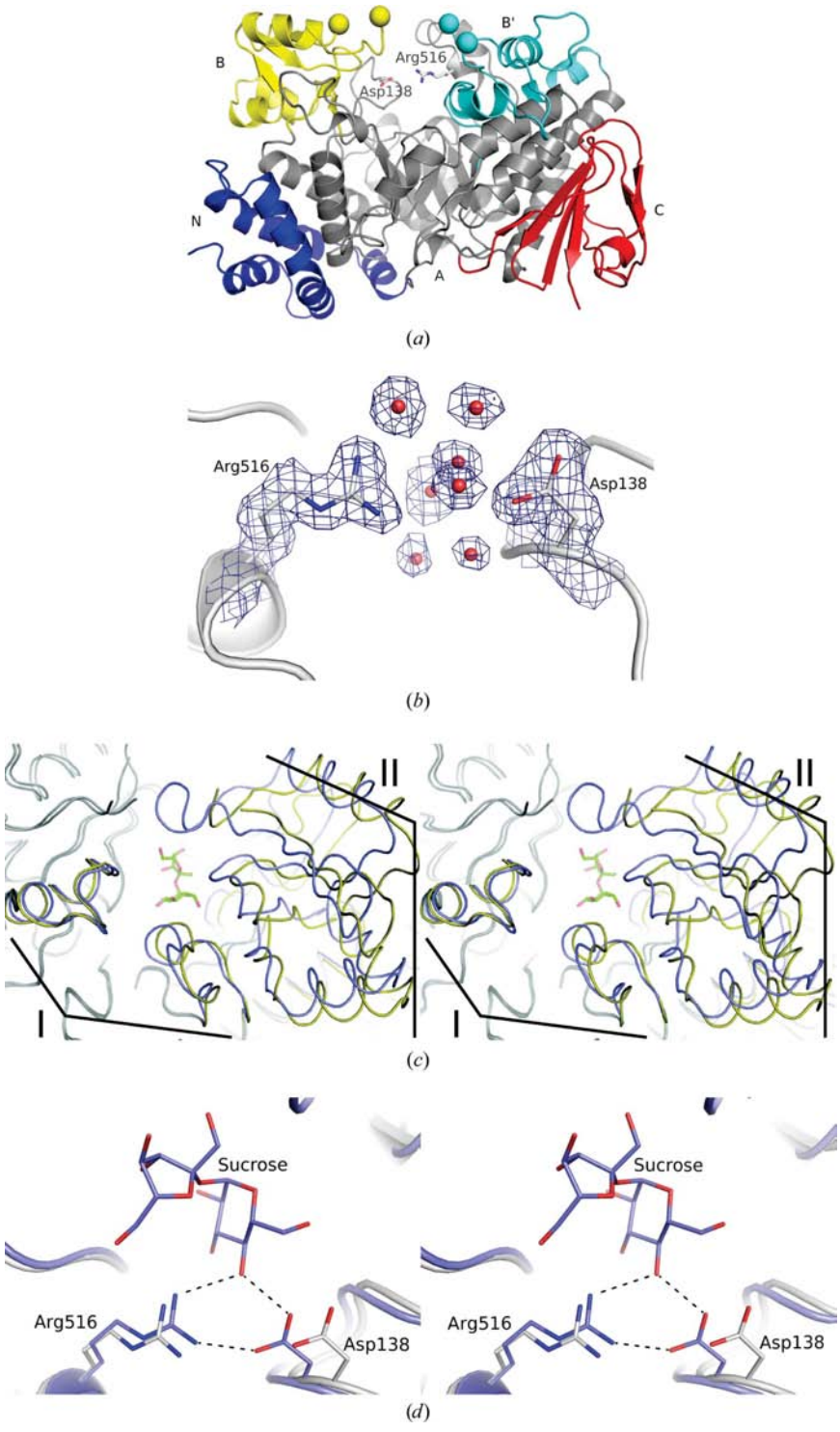

Figure 1
(*a*) Cartoon representation of the apo SC structure. Arg516 and Asp138 are shown in stick representation. The structure consists of five domains: N (blue), A (grey), B (yellow), B′ (cyan) and C (red). The yellow and cyan spheres in domains B and B′ indicate the start and end of the residues missing from the model. (*b*) $2F_o - F_c$ electron-density map contoured at 1σ, shown around the residues Arg516 and Asp138 with water molecules shown as red spheres. (*c*) Superposition of the SX–sucrose complex (PDB code 3czk) with apo SC (enzymes coloured grey and sucrose coloured green). The regions undergoing substrate-induced structural changes, I (apo SC residues 131–146 and 504–518) and II (B domain and apo SC residues 278–308), are indicated by lines and coloured light blue and yellow for SX and apo SC, respectively. (*d*) A close-up stereoview of the superimposed structures of SX–sucrose (light blue) and apo SC (white). The dotted lines between sucrose and the residues indicate hydrogen bonds, as well as a salt bridge between Arg516 and Asp138.

Table 2
Kinetic parameters of sucrose hydrolases.

	Sucrose hydrolases		Amylosucrases	
	SC†	SX‡	ASNp (*Neisseria polysaccharea*)§	ASDr (*Deinococcus radiodurans*)§
Kinetic behaviour	Michaelis–Menten		Modelled by two different Michaelis–Menten equations	
K_m (m*M*)	60.7	2.24	1.90 ([sucrose] < 20 m*M*), 50.20 ([sucrose] > 20 m*M*)	10.00 ([sucrose] < 41 m*M*), 84.00 ([sucrose] > 41 m*M*)
k_{cat} (s^{-1})	21.69	66.45	0.55 ([sucrose] < 20 m*M*), 1.28 ([sucrose] > 20 m*M*)	0.82 ([sucrose] < 41 m*M*), 2.01 ([sucrose] > 41 m*M*)
k_{cat}/K_m (s^{-1} mM^{-1})	0.36	29.66	0.29 ([sucrose] < 20 m*M*), 0.025 ([sucrose] > 20 m*M*)	0.082 ([sucrose] < 41 m*M*), 0.024 ([sucrose] > 41 m*M*)

† This work. ‡ Kim *et al.* (2004). § Potocki de Montalk *et al.* (2000).

3.2. X-ray structure of apo SC

The structure of apo SC consists of 633 residues folded into five domains: the all-helical domain N (residues 5–81), the $(\beta/\alpha)_8$ domain A (residues 82–179, 254–387 and 464–560), domain B (residues 180–253), domain B′ (residues 388–463) and the C-terminal domain C (residues 561–637) (Fig. 1*a*). The apo SC structure provides a view of the enzyme in its resting state, *i.e.* with water molecules occupying subsite −1 (Fig. 1*b*). A comparison of the structure of apo SC with structures of SX shows that apo SC is highly similar to these structures in overall domain size and organization, as expected. The lowest root-mean-square deviation (r.m.s.d.) between apo SC and the SX structures is found when comparing apo SC with the SX–Tris complex (0.45 Å on 507 C^{α} atoms). Tris is known to be a nonbiological competitive inhibitor of some GH-13 enzymes and is thus often found bound in the active site of GH-13 enzymes when used during crystallization (Kim *et al.*, 2008; Skov *et al.*, 2001; Ravaud *et al.*, 2007; Aghajari *et al.*, 1998). Based on the structures it seems that Tris inhibits both SC and SX and locks them in an intermediate conformation between the apo and sucrose-bound conformations.

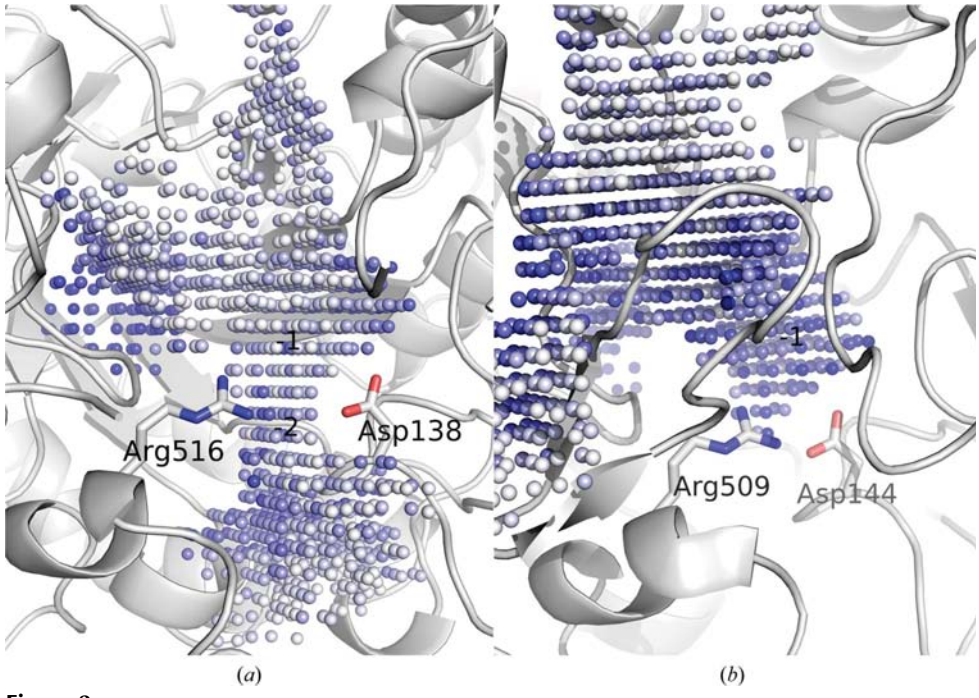

Figure 2
(*a*) The active-site pocket of apo SC illustrated by an ensemble of spheres as calculated using the program *PocketPicker* (Weisel *et al.*, 2007). (*b*) The same for AS (PDB code 1jgi), with sucrose removed from the calculation. The approximate positions of subsites −1 and −2 are labelled. The figure clearly shows that the active-site pocket of apo SC is open to the solvent, whereas that of AS is closed. The colour of the spheres, from white to blue, gives a measure of their burial within the pocket.

3.3. An Arg–Asp charge pair forms in SH upon glucosyl binding

Apo SC is found to be in a more open conformation compared with the SX–sucrose complex (inactive mutant in complex with sucrose), with largest deviations of ∼3.5 Å between corresponding residues (excluding smaller surface-loop movements). These deviations are seen in region I (residues 131–146 and 504–518) and in region II (domain B and residues 278–308) (Fig. 1*c*). The movements observed have clear consequences for the active-site structure: in apo SC subsite −1 is open and extends towards what would be subsite −2 (Fig. 2*a*), *i.e.* from the 'nonreducing' end in, for example, TAKA amylase (Brzozowski & Davies, 1997). In the AS and SX sucrose complexes the binding pocket is closed and does not extend beyond subsite −1 (Fig. 2*b*).

The sucrose-specific enzymes of GH-13 do not require subsites −2, −3 *etc*. The structures of these enzymes show that they all contain an Arg–Asp charge pair in a position that allows interaction through a hydrogen bond with the nonreducing OH (O4) group of the bound glucosyl moiety (Skov *et al.*, 2001; Zhang *et al.*, 2003; Ravaud *et al.*, 2007; Sprogoe *et al.*, 2004; Kim *et al.*, 2008). While forming a hydrogen bond to the O4 atom, the Arg and Asp of the charge pair are also in close proximity (approximately 2.8 Å) to each other and form

a salt bridge. Interestingly, in the structure presented here the Arg516–Asp138 salt bridge is not formed. When comparing the apo SC structure with the ligand-complex structures of SX and AS, a modified active-site conformation of apo SC is seen as a result of the absence of the Arg516–Asp138 salt bridge (a distance of 4.9 Å between the Arg516 NH2 atom and the Asp138 OD1 atom; Fig. 1*d*), leading to a more open active-site binding groove at subsite −1. This observation could have mechanistic implications: the resting enzyme is open for substrate entrance from the direction of the −1/−2 subsite side. Hence, the binding of sucrose and the subsequent formation of the Arg–Asp salt bridge closes the otherwise open active site, a feature that proposes a solution to the sucrose-entrance question for AS.

In the SX and AS structures solved with the inhibitor Tris bound in subsite −1, it is observed that both residues of the Arg–Asp charge pair are involved in interactions with the Tris molecule (Kim *et al.*, 2008; Skov *et al.*, 2001). In the Tris-inhibited SX structure the charge-pair distance is 3.8 Å (between the Arg515 NH1 atom and the Asp137 OD1 atom).

Substrate-mediated salt-bridge formation and subsequent domain movements are not uncommon in nature. α-Glucosidase is another example of an exo-acting enzyme that hydrolyzes nonreducing terminal glucosyl moieties. Superimposition of the α-glucosidase structure and those of AS, SX and apo SC shows that it also contains an Arg–Asp charge pair in the same position as Arg516 and Asp138 (apo SC numbering). To date, the structure of α-glucosidase has been reported in its native apo form only and in this structure the Arg407–Asp60 charge-pair residues are located 10 Å from each other (Shirai *et al.*, 2008). In the periplasmic conformation of lactose permease from *E. coli*, Arg144 has been shown to make a charge pair with Glu126 in the absence of lactose (Abramson *et al.*, 2003). Upon binding of lactose Arg144 shifts from Glu126 to bind the galactosyl moiety of lactose and makes a salt bridge with Glu269, which also interacts with the galactosyl moiety (Mirza *et al.*, 2006). Formation of the Arg144–Glu269 charge pair is believed to trigger the conformational change to the cytoplasmic conformation (Abramson *et al.*, 2003).

3.4. Implications for the GH-13 subfamily 4 enzyme reaction mechanism

The glucosyl binding-mediated salt-bridge formation hypothesis could not previously be validated by structural studies of AS or SH enzymes as it had not been possible to obtain crystals with an empty active site. In addition, this hypothesis had proven to be difficult to address by mutational studies since the residues involved are important for substrate binding to the enzymes. The structure of apo SC with an empty active site and a broken salt bridge thus might provide important clues to further understanding of the GH-13 subfamily 4 enzyme reaction mechanism.

Based on the apo SC structure, we propose an additional conformational change in the SH reaction mechanism: an Arg–Asp salt bridge is formed in the SH and AS enzymes upon binding the glucosyl moiety of sucrose in subsite −1 *via* interactions with the O4 hydroxyl group and this leads to changes in the subsite −1 conformation (Fig. 1*c*). In the case of AS and SC it has so far not been possible to obtain a complex with fructose only occupying the +1 subsite. This could suggest that fructose alone cannot bind in the +1 subsite and must be part of sucrose. In the SHs, binding of sucrose results in a closing movement of the B domain (Fig. 1*c*, region II), with the fructosyl moiety acting as a stabilizer of the closed conformation (Kim *et al.*, 2008). Following formation of the covalent intermediate, the expulsion of fructose most probably occurs *via* opening movements of the B and B′ domains, which would also expose the covalent intermediate and ensure efficient hydrolysis. In contrast, in AS enzymes movement of the B and B′ domains has been observed to be of a much lesser extent and does not provide access to the active site (Skov *et al.*, 2001, 2002; Mirza *et al.*, 2001). This feature, and the assumption that the acceptor glucan remains bound in the channel (subsites +2, +3 and +4) leading to subsite −1, might explain the ability of ASs to elongate efficiently. An opening provided by the broken salt bridge is therefore proposed as an access point for sucrose during elongation.

Kristoffer Rosenstand and Sandra Pizzut are greatly acknowledged for excellent technical assistance, and the EU project CEGLYC is acknowledged for financial support.

References

Abramson, J., Smirnova, I., Kasho, V., Verner, G., Kaback, H. R. & Iwata, S. (2003). *Science*, **301**, 610–615.
Adams, P. D., Grosse-Kunstleve, R. W., Hung, L.-W., Ioerger, T. R., McCoy, A. J., Moriarty, N. W., Read, R. J., Sacchettini, J. C., Sauter, N. K. & Terwilliger, T. C. (2002). *Acta Cryst.* D**58**, 1948–1954.
Aghajari, N., Feller, G., Gerday, C. & Haser, R. (1998). *Structure*, **6**, 1503–1516.
Brunger, A. T. (2007). *Nature Protoc.* **2**, 2728–2733.
Brzozowski, A. M. & Davies, G. J. (1997). *Biochemistry*, **36**, 10837–10845.
Emsley, P. & Cowtan, K. (2004). *Acta Cryst.* D**60**, 2126–2132.
Evans, P. (1993). *Proceedings of the CCP4 Study Weekend. Data Collection and Processing*, edited by L. Sawyer, N. Isaacs & S. Bailey, pp. 114–122. Warrington: Daresbury Laboratory.
Jensen, M. H., Mirza, O., Albenne, C., Remaud-Simeon, M., Monsan, P., Gajhede, M. & Skov, L. K. (2004). *Biochemistry*, **43**, 3104–3110.
Kim, H. S., Park, H. J., Heu, S. & Jung, J. (2004). *J. Bacteriol.* **186**, 411–418.
Kim, M. I., Kim, H. S., Jung, J. & Rhee, S. (2008). *J. Mol. Biol.* **380**, 636–647.
Leslie, A. G. W. (1992). *Jnt CCP4/ESF–EACBM Newsl. Protein Crystallogr.* **26**.
McCoy, A. J., Grosse-Kunstleve, R. W., Adams, P. D., Winn, M. D., Storoni, L. C. & Read, R. J. (2007). *J. Appl. Cryst.* **40**, 658–674.
Mirza, O., Guan, L., Verner, G., Iwata, S. & Kaback, H. R. (2006). *EMBO J.* **25**, 1177–1183.
Mirza, O., Skov, L. K., Remaud-Simeon, M., Potocki de Montalk, G., Albenne, C., Monsan, P. & Gajhede, M. (2001). *Biochemistry*, **40**, 9032–9039.
Pizzut-Serin, S., Potocki-Veronese, G., van der Veen, B. A., Albenne, C., Monsan, P. & Remaud-Simeon, M. (2005). *FEBS Lett.* **579**, 1405–1410.

Potocki de Montalk, G., Remaud-Simeon, M., Willemot, R. M., Sarcabal, P., Planchot, V. & Monsan, P. (2000). *FEBS Lett.* **471**, 219–223.
Ravaud, S., Robert, X., Watzlawick, H., Haser, R., Mattes, R. & Aghajari, N. (2007). *J. Biol. Chem.* **282**, 28126–28136.
Shirai, T., Hung, V. S., Morinaka, K., Kobayashi, T. & Ito, S. (2008). *Proteins*, **73**, 126–133.
Skov, L. K., Mirza, O., Henriksen, A., De Montalk, G. P., Remaud-Simeon, M., Sarcabal, P., Willemot, R. M., Monsan, P. & Gajhede, M. (2001). *J. Biol. Chem.* **276**, 25273–25278.
Skov, L. K., Mirza, O., Sprogoe, D., Dar, I., Remaud-Simeon, M., Albenne, C., Monsan, P. & Gajhede, M. (2002). *J. Biol. Chem.* **277**, 47741–47747.
Sprogoe, D., van den Broek, L. A., Mirza, O., Kastrup, J. S., Voragen, A. G., Gajhede, M. & Skov, L. K. (2004). *Biochemistry*, **43**, 1156–1162.
Sumner, J. B. & Howell, S. F. (1935). *J. Biol. Chem.* **108**, 51–54.
Weisel, M., Proschak, E. & Schneider, G. (2007). *Chem. Cent. J.* **1**, 7.
Zhang, D., Li, N., Lok, S. M., Zhang, L. H. & Swaminathan, K. (2003). *J. Biol. Chem.* **278**, 35428–35434.